

# Testing FLUKA on neutron activation of Si and Ge at nuclear research reactor using gamma spectroscopy

J. Bazo<sup>a</sup>, J.M. Rojas<sup>a</sup>, S. Best<sup>a</sup>, R. Bruna<sup>b</sup>, E. Endress<sup>a</sup>, P. Mendoza<sup>c</sup>, V. Poma<sup>c</sup>, A.M. Gago<sup>a</sup>

<sup>a</sup>*Sección Física, Departamento de Ciencias, Pontificia Universidad Católica del Perú, Av. Universitaria 1801, Lima 32, Perú*

<sup>b</sup>*Cálculo Análisis y Seguridad (CASE), Instituto Peruano de Energía Nuclear (IPEN), Av. Canadá 1470, Lima 41, Perú*

<sup>c</sup>*División de Técnicas Analíticas Nucleares, Instituto Peruano de Energía Nuclear (IPEN), Av. Canadá 1470, Lima 41, Perú*

---

## Abstract

Samples of two characteristic semiconductor sensor materials, silicon and germanium, have been irradiated with neutrons produced at the RP-10 Nuclear Research Reactor at 4.5 MW. Their radionuclides photon spectra have been measured with high resolution gamma spectroscopy, quantifying four radioisotopes ( $^{28}\text{Al}$ ,  $^{29}\text{Al}$  for Si and  $^{75}\text{Ge}$  and  $^{77}\text{Ge}$  for Ge). We have compared the radionuclides production and their emission spectrum data with Monte Carlo simulation results from FLUKA. Thus we have tested FLUKA's low energy neutron library and decay photon scoring with respect to the activation of these semiconductors. We conclude that FLUKA is capable of predicting relative photon peak amplitudes, with gamma intensities greater than 1%, of produced radionuclides with an average uncertainty of 12%. This work allows us to estimate the corresponding systematic error on neutron activation simulation studies of these sensor materials.

*Keywords:* FLUKA, neutron irradiation, nuclear reactor, silicon, germanium

---

## 1. Introduction

At nuclear research facilities semiconductor materials are irradiated with neutrons in order to obtain transmutation doping with high homogeneity. This irradiation method is also used to reproduce radiation damage of active sensors in the context of LHC experiments, among other aims. For instance, there are several studies on neutron irradiation of silicon [1, 2, 3, 4] and germanium [5, 6, 7] detectors.

---

\*Corresponding author

*Email address:* jbazo@pucp.edu.pe (J. Bazo)

Neutron irradiation damage is the consequence of atomic displacements and non-elastic nuclear reactions such as He/H gas production and also solid nuclear transmutation [8]. For example, the atomic displacement alters the microstructure (generating net defects), while the nuclear transmutation changes the chemical composition of materials, modifying in general their properties, such as thermal conductivity and electrical resistivity. In this work, we will focus on the irradiation effects related to nuclear transmutation comparing its measurement with Monte Carlo simulation.

We irradiate different samples of two characteristic semiconductor sensor materials, silicon and germanium, with wide spectrum neutron flux produced at the core of the RP-10 [9] Nuclear Research Reactor at IPEN (Peruvian Institute of Nuclear Energy). Then, we measure their associated radionuclides photon spectra with high resolution gamma spectroscopy.

The Monte Carlo simulation has been performed using FLUKA (FLUktuierende KAskade) [10, 11]. This simulation package describes the radiation interaction and transport in detector materials. In the context of this work, we use FLUKA to estimate the radionuclides production and their emitted gamma spectrum for the neutron irradiation tests already mentioned.

We have carried out a comparison of the experimental data against the FLUKA simulation. A similar FLUKA validation study, [12], irradiated construction materials of high-energy accelerators using the radiation field of a 120 GeV positive hadron beam stopped in a copper target. Thus they explored a higher energy regime and different materials. Our results are in the energy range below 10 MeV and are useful for understanding the accuracy of FLUKA in simulating nuclear solid transmutation as a consequence of neutron irradiation. This serves as benchmark of the low energy neutron library and decay photon scoring.

This paper is divided as follows: we first review the theoretical aspects of the neutron activation analysis. Then, we describe in detail the measurements performed at the nuclear research reactor. Next, we outline the simulation implemented in order to compare it, in the results section, to the experimental data. We conclude estimating the accuracy of FLUKA in predicting the activation products gamma spectrum.

## 2. Neutron Activation Analysis

When a sample is exposed to a high neutron flux in a nuclear reactor core, artificial radionuclides are produced. For instance, in a process referred to as neutron activation, a stable nucleus can absorb (i.e. capture) a free neutron, resulting in an unstable isotope state. The unstable isotope can undergo some de-excitation process reaching a stable nuclide, leading in most cases to observable gamma peaks [13].

A nuclear thermal reactor, as the one we have used, is characterized by its neutron energy spectrum which has three well defined regions: thermal ( $< 1$  eV), epithermal (1 eV - 100 keV) and fast neutrons (100 keV - 10 MeV). The

neutron activation cross section is most relevant in the thermal regime and also for fast neutrons. The corresponding most likely reactions are the capture of thermal neutrons ( $n,\gamma$ ) and the capture of fast neutrons ( $n,p$ ) or ( $n,\alpha$ ).

Other reactions such as ( $n,2n$ ), ( $n,np$ ) and ( $n,d$ ) are not energetically possible below  $\approx 10$  MeV, i.e. the maximum energy of a thermal nuclear research reactor. The neutron activation cross section [14] for each process depends on the target isotope and neutron energy.

The process to follow in order to measure the gamma emission from radionuclides starts by irradiating the sample during a time period, *irradiation time*. Then the gamma spectroscopy measurements begins. During the elapsed time between the end of irradiation and the initial measurement, *decay time*, the radionuclides can decay. Next, the sample is measured in the detector during an interval, *measure time* ( $t_m$ ), when the decaying isotopes are counted. Both irradiation and decay times are input in the FLUKA simulation code.

On the other side, to estimate the corrected total number of emitted photons, from the detected ones, the following factors have to be considered: the detector efficiency  $\epsilon$ , that depends on energy and distance of the source to the detector and the detector's deadtime,  $t_{dead}$ . Then the corrected counting rate  $N$ , given the measured counting rate  $M$ , is:

$$N = \frac{M}{\epsilon} \left( \frac{t_m}{t_m - t_{dead}} \right) \quad (1)$$

### 3. Neutron irradiation measurements

We have irradiated one silicon and two germanium samples followed by measurements with a gamma spectrometer.

#### 3.1. Nuclear Reactor description

The neutron source is the RP-10 [9] Nuclear Research Reactor at IPEN (Peruvian Institute of Nuclear Energy) in Huarangal, near Lima, Peru. The RP-10 is a MTR (Material Testing Reactor) pool-type reactor with  $U_3O_8$  nuclear fuel containing 19.75% enrichment in  $^{235}U$ . The core is located at the bottom of a cylindrical tank (4m diameter and 11m deep) and is surrounded by graphite and beryllium neutron reflectors. The tests were carried out using the same power at 4.5 MW and exposure times of 20 s and 60 s.

The nuclear core configuration number 44 (see Fig. 1) was used. The nominal neutron fluxes measured by activated foil dosimetry at 4.5 MW in the irradiation position A1 (corner of the core grid) at different energy ranges are given in Table 1 with their respective errors. The theoretical neutron spectrum of a thermal reactor was used in the FLUKA simulation, normalized in each energy range with the energy-integrated measured flux given in Table 1. The maximum neutron energy is  $\approx 10$  MeV.

Each sample was stacked into a polyethylene irradiation container. The containers were sent for irradiation using the pneumatic transfer system to the A1 position of the RP-10. Since the irradiation position is at the corner of the

	A	B	C	D	E	F	G	H	I
1	TN	BE	BE	BE	BE	BE	BE	BE	CF
2	GR	BE	CI	NN	NC	NN	BCF	BE	GR
3	BE	BE	NN	AS	A	NC	A	BE	BE
4	BE	BE	A	A	CI	A	A	BE	BE
5	BE	BE	A	NC	A	AS	A	BE	BE
6	GR	BE	CI	NN	A	NN	CI	BE	GR
7	CI	BE	BE	BE	BE	BE	BE	BE	CI
8			GR	GR	GR	GR	GR		

Figure 1: Configuration scheme of RP-10’s 44 core. The codes are: TN (used irradiation position), A and NN (nuclear fuel element), AS and NC (control fuel element), BE(berilium reflector), GR (graphite), CI (irradiation box), BCF (Fine control bar) and CF (fission counter).

core, where the reflectors are located, the flux is no longer isotropic as in the center. A possible error due to this positioning is already taken into account since the neutron flux has been measured at this precise location.

Measured flux	Thermal	Epithermal	Fast
$\times 10^{11}(\text{n/cm}^2\text{s})$	$86 \pm 1.72$	$1.54 \pm 0.15$	$4.59 \pm 0.05$

Table 1: Neutron fluxes estimated using activated foil dosimetry measured at position A1 with 4.5 MW.

### 3.2. Samples description

The silicon and germanium samples are pieces of single side polished (SSP) wafers, 0.5 mm thick, undoped, with  $\langle 100 \rangle$  orientation. Their properties (element, mass), irradiation time and detection specifications (distance to detector, decay time, measurement time and dead time) are summarized in Table 2 showing only the first measurement of each sample.

The chemical composition of the samples was studied previously using SEM-EDX (Scanning Electron Microscope / Energy-Dispersive X-ray) spectroscopy (models FEI Quanta 650 and EDAX TEAM<sup>TM</sup> EDS) with a detection limit of 0.01%. Both silicon and germanium samples were found to have a high purity  $100_{-0.77}^{+0.0}\%$ . In the case of silicon, primary line K and secondary line L were identified and for germanium primary lines  $K\alpha$  and  $K\beta$  as well as secondary line L were singled out.

Element	Mass (mg)	Irradiation time (s)	Distance (mm)	Decay time (s)	Measure time (s)	Dead time (%)
Si	41.38	60	119	202	168.33	7.9
Ge	9.48	20	239	235	205.53	2.7
Ge	11.87	20	239	237	125.61	3

Table 2: Samples irradiation and detection parameters. Only the first measurement of each sample is given. Other measurements performed at different times, included in the analysis, are not listed here.

### 3.3. Gamma spectrometer description

We carried out the spectrum measurements with a High Purity (HP) Ge semiconductor detector: ORTEC model GEM70P4 (70% relative efficiency and 1.9 keV resolution (FWHM) for the 1332.5 keV peak of  $^{60}\text{Co}$  and 1 keV resolution at 122 keV). For each sample several gamma spectroscopy measurements were performed at different times. Measurements were done using a 3D-printer sample holder with custom made geometry such as to minimize the gamma attenuation.

The efficiency of the spectrometer, including error bands, as a function of the energy at the two measurement distances are shown in Fig.2. The function is a 4-degree polynomial fit to the efficiency data. The efficiency calibration has been performed from 100 keV to 1800 keV, thus energies outside this range have a much higher uncertainty. This detection efficiency correction is applied afterwards in order to account for the gamma spectroscopic measurement specific characteristics not described in the simulation.

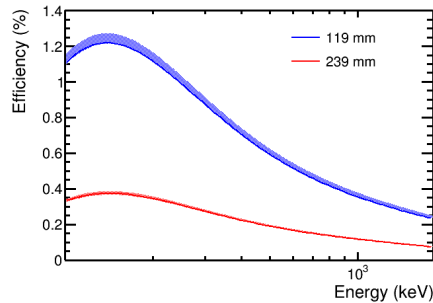


Figure 2: Efficiency of ORTEC model GEM70P4 spectrometer used at two different detection distances. The shadowed bands represent the estimated error.

Under the conditions described above, the peaks and radionuclides product of the nuclear reactions and decays were determined. We have worked with a deadtime lower than 8% and 5%, for silicon and germanium respectively, in order to maintain the pulse shaping formation. However, as a side effect we get lower statistics for some gamma peaks that are later removed, as mentioned in Sec. 5.

## 4. FLUKA simulation implementation

We have performed FLUKA simulations for a simplified description of the experiment. The samples are exposed to a direct and collimated neutron beam that follows the spectrum of the RP-10 reactor. Then the photon spectrum emitted by the radioactive nuclides is recorded.

The coded geometry resembles that of the samples. Each material (i.e. silicon and germanium) is defined with the appropriate natural isotope abundances.

A user-defined source routine was implemented for the neutron energy spectrum of the RP-10 from tabulated data of the flux described in Sec. 3.1. In order to represent the irradiation, a 1cm-radius circular neutron beam is used pointing 0.01 mm off in the z axis towards the center of the sample, hitting it perpendicularly to its longitudinal section.

The simulation defaults have been set to *precision* activating the corresponding flag. In addition, the simulation of radioactive decays (RADDECAY) has been activated. The irradiation profile (IRPROFI) for radioactive decays uses the irradiation intervals given in Table 2 with an equivalent beam intensity of  $\approx 2.9 \times 10^{13}$  neutrons/s (total energy integrated flux in the beam area).

In order to improve statistics, each radioactive nucleus is *decayed* in 10 replicas. We used the activation study mode where the time evolution is calculated analytically and all daughter nuclei and associated radiation are considered at fixed experimental decay times (DCYTIMES) given in Table 2. At these times after irradiation, decay photons from radioactive products are scored (DCYSCORE) over a spherical region surrounding the sample. The measurement duration is introduced analytically after simulation using Eq.2.

In addition, residual nuclei, produced in the inelastic interactions inside the nuclear reactor, have been scored (RESNUCLEI) in all regions in order to compare them with the expected radionuclides to be observed.

For both materials independent simulations were performed with  $10^9$  primary particles.

## 5. Validation results

The gamma spectrometer measurements of the samples were performed in the energy range from 39 keV to 3223 keV. The nuclide and peak analysis report is given in Table 4.

In general, silicon has three natural occurring isotopes:  $^{28}\text{Si}$ ,  $^{29}\text{Si}$  and  $^{30}\text{Si}$ , with average relative isotope abundances of 92.2, 4.7 and 3.1%, respectively [15]. These isotopes can undergo the three main processes ((n, $\gamma$ ), (n,p) and (n, $\alpha$ )) for neutron capture. Out of the nine possible outcomes, only five reach radioactive nuclides ( $^{31}\text{Si}$ ,  $^{28}\text{Al}$ ,  $^{29}\text{Al}$ ,  $^{30}\text{Al}$  and  $^{27}\text{Mg}$ ). However,  $^{30}\text{Al}$  is hardly observable since its half-life is 3.6s. The cross sections for  $^{30}\text{Si} \rightarrow (\text{n,p})^{30}\text{Al}$  and  $^{30}\text{Si}(\text{n},\alpha) \rightarrow ^{27}\text{Mg}$  are only important at higher energies, hardly achievable by the nuclear research reactor due to its low flux. In the case of  $^{30}\text{Si}(\text{n},\gamma) \rightarrow ^{31}\text{Si}$ , even if the cross section and the neutron flux are high at low energies, the gamma intensity of the related peak is very low (0.055%), thus the expected number of counts is low. Therefore only two radioactive nuclides, shown in Table 4, have been observed:  $^{28}\text{Al}$  and  $^{29}\text{Al}$ .

Germanium has five natural isotopes:  $^{70}\text{Ge}$ ,  $^{72}\text{Ge}$ ,  $^{73}\text{Ge}$ ,  $^{74}\text{Ge}$  and  $^{76}\text{Ge}$ , with average relative isotope abundances of 20.84, 27.54, 7.73, 36.28 and 7.61%, respectively [15]. These isotopes can undergo neutron capture reactions via the same three main processes. There are fifteen possible outcomes, however, the reaction cross sections of (n,p) and (n, $\alpha$ ) are almost three orders of magnitude

Silicon products			
A	12 (Mg)	13 (Al)	14 (Si)
25	28.03 ± 0.05		
26	1.72 ± 0.01		
27	0.153 ± 0.004		
28		42.08 ± 0.05	100.00 ± 0.09
29		1.47 ± 0.01	5.14 ± 0.01
30		0.029 ± 0.001	5.62 ± 0.02
31			0.0016 ± 0.0003
Germanium products			
A	30 (Zn)	31 (Ga)	32 (Ge)
67	$(5.3 \pm 0.5) \times 10^{-2}$		
69	$(2.0 \pm 0.8) \times 10^{-3}$		
70	≈ 0	$(5.0 \pm 0.4) \times 10^{-2}$	9.08 ± 0.05
71			44.43 ± 0.13
72		$(2.7 \pm 1.0) \times 10^{-3}$	14.09 ± 0.06
73		≈ 0	22.16 ± 0.10
74			100.00 ± 0.19
75			13.22 ± 0.05
76			4.38 ± 0.03
77			0.89 ± 0.02

Table 3: Residual nuclei, by atomic number and mass number (A), estimated with FLUKA for the silicon and germanium samples. Values have been normalized to the maximum of each sample.

below the highest  $(n,\gamma)$  reaction, compared to just one order of magnitude difference in the case of silicon. Therefore all  $(n,p)$  and  $(n,\alpha)$  reactions are suppressed and only  $(n,\gamma)$  is favoured. There are five such cases, of which only three lead to radioactive nuclides ( $^{71}\text{Ge}$ ,  $^{75}\text{Ge}$  and  $^{77}\text{Ge}$ ). From these  $^{71}\text{Ge}$  is not observable since it has one decay mode ( $T_{1/2}=11.4$  days) which only emits X-rays that cannot be detected with the gamma spectrometer. The other decay is metastable with  $T_{1/2}=20\text{ms}$  and even if it emits 174.9 keV photons it has already disappeared by the time a spectroscopic measurement can be done. Thus only two radioactive nuclides, shown in Table 4, are observed:  $^{75}\text{Ge}$  and  $^{77}\text{Ge}$ .

The expected produced radioactive nuclides described above are in agreement with the residual nuclei results from FLUKA shown in Table 3.

Some important comments are in order. We have neglected the metastable signatures and the peaks with gamma intensity lower than 1%, in order to make a fair comparison with FLUKA. We exclude the metastable decays ( $^{74}\text{Ge}(n,\gamma) \rightarrow ^{75m}\text{Ge}$ ,  $t_{1/2}=47.7\text{s}$  and  $^{76}\text{Ge}(n,\gamma) \rightarrow ^{77m}\text{Ge}$ ,  $t_{1/2} = 53.7\text{s}$ ) since the uncertainty in the measured time interval compared to the half-life introduces a much larger error. The gamma intensity cut is at the limit of detection capabilities, removing six peaks of  $^{75}\text{Ge}$  and two peaks of  $^{77}\text{Ge}$ . In addition, identified background peaks are not reported in these results. These peaks correspond to the  $K_\alpha$  and

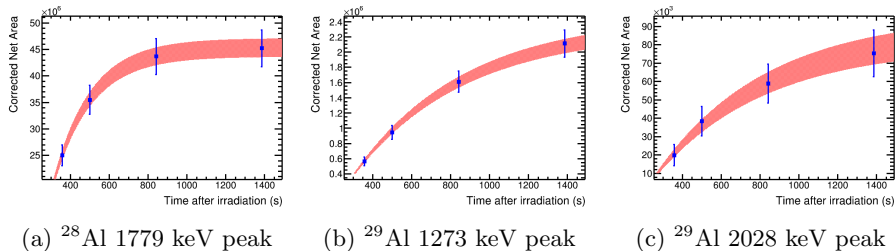


Figure 3: Time evolution of spectrometer measurements with theoretical fitting for silicon products. The shadowed band represents the error of the fit. Points are drawn at the end of the measurement and include the decay time.

$K_\beta$  characteristic X-rays emitted by lead from the detector shielding, a peak from electron-positron pair annihilation, peaks from double and single escapes, sum peaks and also  $^{40}\text{K}$  natural background radiation.

In order to make a direct comparison between the FLUKA simulation results with those from the neutron irradiation measurements, we have corrected the effects of the spectrometer in the latter by dividing the net area of each peak by its efficiency at the given energy (see Fig. 2) and by the uptime fraction (see Table 2). The total error on the measurements, displayed in Table 4, encloses the uncertainties in the net area and in the detector efficiency. The total simulation uncertainty is given by adding in quadrature the statistical error, a 1-2% error on the mean value, due to the neutron flux, and the normalization error in the photon peaks, that we explain below.

The FLUKA photon peak amplitudes are normalized by a single constant for each sample that minimizes the difference between simulation and experimental measurement, thus only relative peak amplitudes will be compared.

This procedure is done as follows: first, for each energy peak, the time evolution of data during the measurements is fitted with the following function:

$$N_0 \left( e^{-\frac{t-t_0}{\tau}} - e^{-\frac{t}{\tau}} \right) \quad (2)$$

where  $N_0$  is the starting number of radionuclides,  $t_0$  is the starting time of the measurement and  $\tau$  is the lifetime of the radionuclide. From the fit we extract  $N_0$  which we will compare with the one obtained using the FLUKA simulation. As an example of these fits, we show in Fig. 3 the results for the silicon sample.

Next we compare each  $N_0$  obtained from the measurements with the simulation results from FLUKA. Assuming no variation in the nuclides natural abundances, the ratio  $N_0^{data}/N_0^{sim}$  for each radionuclide should be a constant for all peaks for the same sample. Then the global normalization for the FLUKA photon peaks amplitudes is obtained by the error-weighted average of the ratios constants ( $N_0^{data}/N_0^{sim}$ ) of the different energy peaks.

In Fig. 4a and 4b the gamma spectrum of neutron-activated silicon and germanium comparing experimental data with FLUKA simulation is presented. The full results, including the capture reaction, half-life, peak energy and gamma

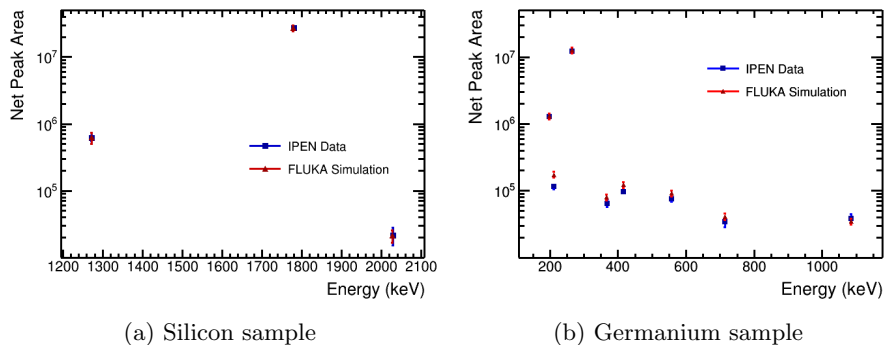


Figure 4: Gamma spectrum of neutron activated samples comparing experimental measurements and FLUKA simulations for peaks with intensities greater than 1% and non metastable decays. The Si sample was irradiated for 60 s at 4.5 MW and the counts collected for 168.33 s after 202 s decay time. The Ge sample was irradiated for 20 s at 4.5 MW and the counts collected for 205.53 s after 235 s decay time.

intensity, are given in Table 4 where the difference between data and simulation is given in terms of sigmas ( $\frac{|N_{exp} - N_{sim}|}{\sqrt{\sigma_{exp}^2 + \sigma_{sim}^2}}$ ). The average difference for both materials in photon peak amplitude is  $0.8 \sigma$ . We also observe that FLUKA is capable of predicting relative peak amplitudes of produced radionuclides with an average uncertainty of 12%, evaluated with  $\frac{|N_{exp} - N_{sim}|}{N_{sim}} \times 100\%$ . It is worth mentioning that the validation results for silicon are very accurate with an uncertainty of less than 2%. The average total error on the measurement is 11.5% and on the simulation 14.7%, while for the simulation it is mostly driven by the error on the normalization, for the experimental data it is due to the uncertainty in the detector efficiency and the statistical error of the counts.

Nuclide	Abundance (%)	Half-life	IAEA energy (keV)	Measured energy (keV)	IAEA intensity	Corr† Net Peak Area	Error stat+syst (%)	FLUKA sim*	Error stat+syst (%)	$\sigma$
$^{28}\text{Si}(n,p) \rightarrow ^{28}\text{Al}$	92.2	2.24min	1778.99	1780.09±2.0	100	$2.71 \times 10^7$	7.8	$2.71 \times 10^7$	12.2	0
$^{29}\text{Si}(n,p) \rightarrow ^{29}\text{Al}$	4.7	6.56min	1273.36	1273.22±1.8	91.3	$6.12 \times 10^5$	10	$6.26 \times 10^5$	20.2	0.1
			2028.1	2029.09±2.1	3.5	$2.16 \times 10^4$	28.8	$2.13 \times 10^4$	22.3	0.04
$^{74}\text{Ge}(n,\gamma) \rightarrow ^{75}\text{Ge}$	36.28	82.78m	198.6	198.89±1.07	1.19	$1.27 \times 10^6$	4.1	$1.3 \times 10^6$	13.2	0.18
$^{76}\text{Ge}(n,\gamma) \rightarrow ^{77}\text{Ge}$	7.61	11.211h	211.03	211.30±1.08	30	$1.16 \times 10^5$	8.5	$1.74 \times 10^5$	13.3	2.33
			367.49	367.71±1.24	14.5	$6.46 \times 10^4$	10.2	$8.04 \times 10^4$	13.4	1.23
			416.35	416.72±1.29	22.7	$9.57 \times 10^4$	8.5	$1.23 \times 10^5$	13.4	1.5
			557.92	558.40±1.40	16.8	$7.57 \times 10^4$	10.2	$9.19 \times 10^4$	13.4	1.11
			714.37	714.73±1.50	7.5	$3.39 \times 10^4$	17.0	$4.11 \times 10^4$	13.6	0.89
			1085.23	1085.79±1.71	6.4	$3.80 \times 10^4$	17.8	$3.46 \times 10^4$	13.8	0.41
Combined peaks $^{75}\text{Ge} + ^{77}\text{Ge}$			264.6/264.45	264.97±1.14	11.4/53.3	$1.21 \times 10^7$	3.1	$1.27 \times 10^7$	13.2	0.37

Table 4: Validation results for Si and Ge comparing experimental measurements (ORTEC spectrometer model GEM70P4) and FLUKA simulations for the main gamma peaks from nuclide decays. †Corrected for efficiency and uptime. \*FLUKA simulation results are normalized as described before.

The last column represents the difference between experiment and simulation as a number of standard deviations:  $\frac{|N_{exp} - N_{sim}|}{\sqrt{\sigma_{exp}^2 + \sigma_{sim}^2}}$

## 6. Conclusions

FLUKA has been confirmed to give reliable results for neutron activation of two semiconductor materials, silicon and germanium, in reactor experiments. Since the nuclear research reactor energies are below 10 MeV, we have tested FLUKA's low energy neutron library that predicts the corresponding cross sections for all interactions. In addition, the decay photon scoring reproduces the expected counts in the gamma spectrometer.

The gamma emitted spectrum of radionuclides produced by these materials irradiated at a nuclear research reactor has been measured using a high purity Ge gamma spectrometer. These results have been compared to the predictions from FLUKA obtaining a mean agreement within 12% for the intermediate-lived radioisotopes and peaks with gamma intensities greater than 1%. In the case of silicon, the accuracy is higher, with an uncertainty lower than 2%.

Simulating with high reliability the neutron transmutation of semiconductors is useful in doping studies, as well as in evaluating the radiation damage, since part of it is due to the change in the chemical composition of the active sensor, altering its properties. These type of studies have an important impact given the coming upgrade of different LHC experiments subdetectors, which base their detection technology on semiconductor sensors.

## 7. Acknowledgments

The authors gratefully acknowledge DGI-PUCP for financial support under Grant No. DGI-2015-192, as well as CONCYTEC under Grant No. FONDECYT-2013-102. The authors wish to thank the FLUKA scientific committee for useful comments and suggestions.

## References

- [1] L. Viererbl, et al., Radiation measurements after irradiation of silicon for neutron transmutation doping, *Rad. Phys. Chem.* 95 (2014) 389–391. doi:10.1016/j.radphyschem.2012.12.024.
- [2] C. Bosetti, et al., Systematic study of neutron irradiation effects on the performance of FZ and MCZ silicon detectors, *Nuc. Instr. Meth. Phys. Res. A* 345 (1994) 250–255. doi:10.1016/0168-9002(94)90998-9.
- [3] F. Lemeilleur, et al., Neutron, proton, and gamma irradiations of silicon detectors, *IEEE Trans. Nucl. Sci.* 41 (1994) 425–431.
- [4] F. Ahmadov, Irradiation tests and expected performance of readout electronics of the ATLAS hadronic endcap calorimeter for the HL-LHC, *J. Instrum.* 9 (2014) C01028. doi:10.1088/1748-0221/9/01/C01028.
- [5] H. W. Kraner, R. H. Pehl, E. E. Haller, Fast neutron radiation damage of high-purity germanium detectors, *IEEE Trans. Nuc. Sci.* 22 (1975) 149–159. doi:10.1109/TNS.1975.4327633.

- [6] P. Marshall, C. Dale, E. Wolicki, Proton, neutron and electron -induced displacement damage in germanium, *IEEE Trans. Nuc. Sci.* **36** (1989) 1882–1888. doi:10.1109/23.45382.
- [7] S. Mathimalar, et al., Study of radioactive impurities in neutron transmutation doped germanium, *Nuc. Instr. Meth. Phys. Res. A* **774** (2015) 6873. doi:10.1016/j.nima.2014.11.056.
- [8] M. Sawan, L. Snead, S. Zinkle, Radiation damage parameters for SiC/SiC composite structure in fusion nuclear environment, *Fusion Sci. Tech.* **44** (2003) 150–154. doi:10.13182/FST03-A325.
- [9] O. Anaya, R. Arrieta, W. Castillo, J. Villanueva, A. Urcia, Operation and use of the RP-10 reactor, *Tech. Rep. INIS-PE-039, IPEN* (2002).
- [10] T. Bohlen, et al., The FLUKA code: Developments and challenges for high energy and medical applications, *Nuclear Data Sheets* **120** (2014) 211–214. doi:10.1016/j.nds.2014.07.049.
- [11] A. Fasso, et al., FLUKA: a multi-particle transport code, in: *CERN 2005-10* (2005), INFN/TC 05/11, SLAC-R-773, 2005. doi:10.2172/877507.
- [12] M. Brugger, A. Ferrari, S. Roesler, L. Ulrici, Validation of the FLUKA Monte Carlo code for predicting induced radioactivity at high-energy accelerators, *Nuc. Instr. Meth. Phys. Res. A* **562** (2006) 814–818. doi:10.1016/j.nima.2006.02.062.
- [13] M. Bhat, et al., NNDC On-Line Data Service from the Evaluated Nuclear Structure Data File Database (2016).  
URL <http://www.nndc.bnl.gov/ensdf/>
- [14] NNDC Sigma Evaluated Nuclear Data File (ENDF) (2016).  
URL <http://www.nndc.bnl.gov/sigma/>
- [15] K. Rosman, P. Taylor, Isotopic composition of the elements 1997, *Tech. Rep. 70, 217-235, Int. Union Pure Appl. Chem.* (1998).